Regulation of Transcription of the *Bacillus subtilis pyrG* Gene, Encoding Cytidine Triphosphate Synthetase

QI MENG AND ROBERT L. SWITZER*

Department of Biochemistry, University of Illinois, Urbana, Illinois 61801

The *B. subtilis pyrG* gene, which encodes CTP synthetase, is located far from the pyrimidine biosynthetic operon on the chromosome and is independently regulated. The *pyrG* promoter and 5′ leader were fused to *lacZ* and integrated into the chromosomes of several *B. subtilis* strains having mutations in genes of pyrimidine biosynthesis and salvage. These mutations allowed the intracellular pools of cytidine and uridine nucleotides to be manipulated by the composition of the growth medium. These experiments indicated that *pyrG* expression is repressed by cytidine nucleotides but is largely independent of uridine nucleotides. The start of *pyrG* transcription was mapped by primer extension to a position 178 nucleotides upstream of the translation initiation codon. A factor-independent termination hairpin lying between the *pyrG* promoter and its coding region is essential for regulation of *pyrG* expression. Primer-extended transcripts were equally abundant in repressed and derepressed cells when the primer bound upstream of the terminator, but they were much less abundant in repressed cells when the primer bound downstream of the terminator. Furthermore, deletion of the terminator from *pyrG-lacZ* fusions integrated into the chromosome yielded elevated levels of expression that was not repressible by cytidine. We suggest that cytidine repression of *pyrG* expression is mediated by an antitermination mechanism in which antitermination by a putative *trans*-acting protein is reduced by elevated levels of cytidine nucleotides. Conservation of sequences and secondary structural elements in the *pyrG* 5′ leaders of several other gram-positive bacteria indicates that their *pyrG* genes are regulated by a similar mechanism.

The regulation of transcription of the *Bacillus subtilis pyr* operon, which encodes the enzymes of de novo UMP biosynthesis, has been extensively studied in this laboratory (for a review, see reference 31). Expression of this operon is governed by a transcriptional attenuation mechanism. When uridine nucleotide levels are elevated in the cells, the protein encoded by the first gene in the operon, PyrR, acts to promote termination of transcription at three attenuation sites located in the 5′ end of the operon. PyrR brings about termination by binding to *pyr* mRNA at specific sites and altering its secondary structure such that formation of a downstream transcription terminator is favored.

By contrast, very little is known about the regulation of expression of *pyrG*, the gene encoding CTP synthetase, in *B. subtilis* or other bacteria. The *pyrG* gene is not part of the *pyr* operon in *B. subtilis*. The gene was identified by Trach et al. (32), who called it *ctrA*, as a gene lying between *rpoE*, which encodes the δ subunit of RNA polymerase, and *spo0F*. Expression of *B. subtilis pyrG* is not coordinated with that of the *pyr* operon. This conclusion comes from the experiments of Asahi et al. (3), who showed that in wild-type cells both uridine and cytidine repressed the *pyr* operon enzymes but not CTP synthetase. In a cytidine deaminase-deficient mutant, which cannot convert cytidine to uridine, cytidine was able to repress CTP synthetase but was no longer able to repress genes of the *pyr* operon. These results suggest that repression of the *pyr* operon is brought about by uridine nucleotides, in accord with our present understanding of the system (31), but that *pyrG* is

specifically repressed by cytidine nucleotides. Nothing is known about the mechanism of this repression.

The only other study of the regulation of bacterial *pyrG* of which we are aware is that of West and O'Donovan (36). These authors reported that repression of *pyrG* by cytidine could be demonstrated only in a *Salmonella enterica* serovar Typhimurium strain in which the cytidine deaminase gene *cdd* was inactive and in which a leaky UMP kinase (*pyrH*) gene brought about abnormally low levels of pyrimidine nucleoside di- and triphosphates. Again, no information about the mechanism of this repression is available.

In the present study we identified the site of transcriptional initiation for *B. subtilis pyrG*. We showed that repression is responsive to cytidine nucleotide levels and is independent of both uridine nucleotides and PyrR-dependent attenuation. To do this, it was necessary to determine *pyrG* expression in mutant strains in which nucleotide pools could be manipulated by blockage of the de novo biosynthetic pathway (using *pyrB* and *pyrDII* mutants) or by inactivation of genes involved in interconversion of uridine and cytidine nucleotides (using *cdd* and *pyrG* mutants) (Fig. 1). Primer extension analysis and mutational analysis of the *pyrG* 5′ leader indicates that repression is brought about by a transcriptional antitermination mechanism that involves an attenuator lying between the *pyrG* promoter and its coding region.

MATERIALS AND METHODS

Bacterial strains, plasmids, media, and growth conditions. Bacterial strains used in this study are listed in Table 1. LB medium (22) was used as the rich liquid medium and the solid medium (1.5% agar) for both *Escherichia coli* and *B. subtilis*. Buffered minimal medium (19) was used as the chemically defined growth medium. Histidine (50 μg/ml) was used for growth of *B. subtilis* strain DB104 and its derivatives. To starve *B. subtilis* strain HC11 for pyrimidines, 100 μg of orotate per ml was used. To grow *B. subtilis* in the presence of excess

* Corresponding author. Mailing address: Department of Biochemistry, University of Illinois, 600 South Mathews Ave., Urbana, IL 61801. Phone: (217) 333-3940. Fax: (217) 244-5858. E-mail: rswitzer@uiuc.edu.
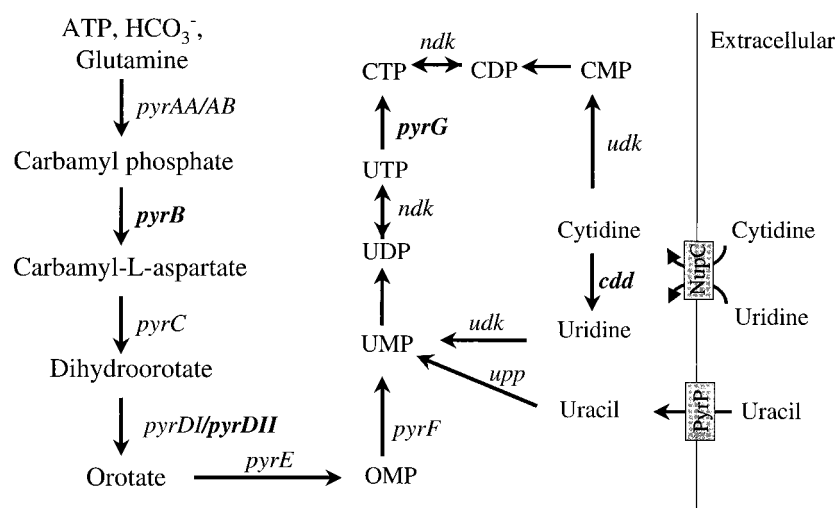
FIG. 1. Genes for pyrimidine nucleotide metabolism in *B. subtilis*. Known pathways for de novo biosynthesis and salvage are shown. Transport proteins implicated in uptake of pyrimidines are indicated by shaded boxes. Genes that were disrupted in strains used in this study to characterize the repression of *pyrG* are indicated in boldface.

pyrimidines, either 50 μg of uracil per ml plus 50 μg of uridine per ml or 200 μg of cytidine per ml was used. For selection of antibiotic resistance, antibiotics were used at the following concentrations: sodium ampicillin, 100 μg/ml; chloramphenicol, 6 μg/ml for *B. subtilis* and 20 μg/ml for *E. coli*; spectinomycin, 100 μg/ml; erythromycin 1 μg/ml.

Bacterial transformation, isolation, manipulation, and analysis of DNA and RNA. Transformation of *E. coli* was carried out as described by Sambrook et al. (26). Transformation of *B. subtilis* followed the procedure of Contente and Dubnau (6).

Plasmid DNA from *E. coli* was isolated as described by Sambrook et al. (26) and purified using the plasmid Miniprep kit from Qiagen. *B. subtilis* chromosomal DNA was isolated by the protocol of Wilson (37). PCR was performed with Vent$_R$ or *Taq* DNA polymerase in a Perkin-Elmer Cetus DNA thermal cycler by the procedure recommended by the manufacturer. DNA sequencing was done at the Genetic Engineering facility in the University of Illinois Biotechnology Center.

Total RNA was extracted from *B. subtilis* according to the method of Saxild et al. (29). Cells were harvested in exponential phase at a cell density of approximately 90 Klett units except for strain HC11 grown on orotate and DB104 *pyrG*::*erm* grown with limiting cytidine, which were harvested at 60 to 65 Klett units. To remove DNA from total RNA samples, the DNA-free kit from Ambion was used as recommended by the supplier.

Strain constructions. *B. subtilis* strain DB104 Δ*pyrDIIcdd* was constructed as follows. Plasmid pMutin was digested with *Bcl*I. The 5.9-kb fragment was gel purified and religated, yielding plasmid pHV502, which lacks the *lacI* gene and part of *lacZ*. A 186-bp fragment from the *cdd* gene was amplified from *B. subtilis* chromosomal DNA by PCR using primers cddHindIII and cddBamHI (Table 2). The PCR product was digested with *Hind*III and *Bam*HI and ligated to *Hind*III-BamHI-digested pHV502 to form plasmid pMX. pMX DNA was introduced into strain DB104 Δ*pyrDII* by transformation, selecting for erythromycin resistance. *B. subtilis* strain DB104 *pyrG*::*cm* was constructed by transforming *Nde*I-linearized pJH4521 into DB104, selecting for chloramphenicol resistance, and confirming that the transformants were auxotrophic for cytidine. The *B. subtilis* strain DB104 *pyrG*::*erm* was constructed by transforming plasmid pCm::Er into DB104 *pyrG*::*cm*.

Construction and integration of *pyrG-lacZ* fusion integrant strains. The integration plasmids listed in Table 1 were constructed by PCR amplification of fragments containing the desired region of *pyrG* using plasmid pJH4133 as the template. The PCR fragments were digested with *Eco*RI and *Bam*HI and ligated into *Eco*RI- and *Bam*HI-digested pDH32. The primers used in making each construct are listed in Table 2 as pyrG-A through pyrG-H. For each of the integration plasmids, the last two letters of the name (Table 1) indicate the primers from this series used to construct it. However, pMSANMF was constructed through several steps. First, −96 to +20 of the *pyrG* sequence was amplified by PCR with primers pyrG-A and pyrG-N. This PCR fragment was digested with *Eco*RI and *Sac*I and ligated to *Eco*RI-*Sac*I-digested pUC19 to form pUCAN. Then, +30 to +218 of the *pyrG* sequence was amplified by PCR

with primers pyrG-M and pyrG-F. After digestion with *Sac*I-*Bam*HI, this PCR product was ligated to *Sac*I-*Bam*HI digested pUCAN to form pUCANMF. Because of the overhang and restriction site introduced, nucleotides +21 to +29 of the *pyrG* 5′ leader sequence were substituted as shown in Fig. 6. A 0.32-kb *Eco*RI-*Bam*HI fragment of pUCANMF was subcloned into pDH32 to form pMSANMF.

pyrG-lacZ fusion integrant strains were constructed as previously described (33). The integration plasmids were linearized with *Sca*I and *Pst*I and transformed into *B. subtilis*. Transformants were selected for chloramphenicol resistance, and disruption of *amyE* was verified on 1% starch–LB plates.

Primer extension, Northern hybridization, and RT-PCR. Primer extension was performed as described by Saxild et al. (29). Reverse transcription (RT) reactions with avian myeloblastosis virus reverse transcriptase (Promega) were incubated at 42°C for 1 h with 10 μg of total RNA and either primer C or primer B (Table 2). The DNA sequencing ladder used for analysis of primer extension was generated by the dideoxynucleotide method of Sanger et al. (27) using the T7 Sequenase v2.0 DNA sequencing kit (Amersham Life Science) and plasmid pJH4133 as the template.

Northern blot analysis was performed with a modification of the method of Nygaard et al. (24). RNA was separated on a 1.5% agarose gel and transferred to a BrightStar-Plus positively charged nylon membrane (Ambion). After transfer, RNA was cross-linked to the membrane by a UV cross-linker. ULTRAhybe hybridization buffer (Ambion) was used for hybridization. The DNA probes for Northern blot analysis were generated by standard PCR except that unlabeled dCTP was used at 1 μM and [α-^{32}P]dCTP was added at 0.16 μM and a total radioactivity of 50 μCi. Plasmid pJH4133 was used as the template, and pyrG-O and pyrG-P were used as primers for labeling the *pyrG* probe. *Eco*RI-*Hind*III digested pFL32 was used as the template, and rpoE-A and rpoE-B were used as primers for labeling the *rpoE* probe.

RT-PCR was performed using Superscript II RNase H$^-$ reverse transcriptase (Gibco BRL) for RT as recommended by the supplier. Total RNA (0.2 μg) treated with DNase I and 5 ng of primer per μl were used. Two of the 20 μl of RT reaction mixture was used for PCR. *Taq* polymerase (Gibco BRL) was used for PCR. Plasmid pJH4133 was used as the template for the positive PCR control. Reverse transcriptase was omitted from the normal reaction to provide a negative control. The primers used for RT-PCR are listed in Table 2.

Enzymatic assays. β-Galactosidase activity was determined by a protocol (19) modified from Miller's method (22). The data in Table 3 are the averages of at least six determinations with the indicated standard deviations. Cells were harvested for assay in the exponential phase of growth at a density of about 90 Klett units, except for slowly growing derivatives of strain HC11 grown on orotate or QM206 grown with limiting cytidine, which were harvested at a density of 35 to 65 Klett units.

Unpublished DNA sequence data. Preliminary sequence data for portions of the *pyrG* genes from several bacteria listed in Fig. 7 were obtained from The Institute for Genomic Research (TIGR) at http://www.tigr.org.

TABLE 1. Bacterial strains and plasmids used in this study

Strain	Genotype or description	Source (reference)
Strains		
E. coli DH5α	Φ80d*lacZ*ΔM15 *recA1 endA1 gyrA96 thi-1 hsdR17*(r_K^- m_K^+) *supE44 relA1 deoR* Δ(*lacZYA-argF*)*U169*	Laboratory stock
B. subtilis		
DB104	*his nprR2 nprE18* Δ*aprA3*	Laboratory stock
DB104Δ*pyrR*	HC11 *pyrB*$^+$ Spec^s Δ*pyrR*	Tumer et al. (33)
DB104Δ*pyrDII*	DB104 Δ*pyrDII*	Kahler and Switzer (14)
HC11	DB104 *pyrB*::Spec^r	Hu and Switzer (11)
DB104Δ*pyrDIIcdd*	DB104 Δ*pyrDII cdd*::pMX	This study
DB104*pyrG*::*cm*	DB104 *pyrG*::Cm^r	This study
DB104*pyrG*::*erm*	DB104 *pyrG*::Erm^r	This study
QM201	DB104 *amyE*::pMSAF	This study
QM202	DB104 Δ*pyrR amyE*::pMSAF	This study
QM203	DB104 Δ*pyrDII amyE*::pMSAF	This study
QM204	DB104 Δ*pyrDIIcdd amyE*::pMSAF	This study
QM205	HC11 *amyE*::pMSAF	This study
QM206	DB104 *pyrG*::*erm amyE*::pMSAF	This study
QM102	HC11 *amyE*::pMSAD	This study
QM103	HC11 *amyE*::pMSAH	This study
QM104	HC11 *amyE*::pMSAB	This study
QM105	HC11 *amyE*::pMSCD	This study
QM234	DB104 Δ*pyrDIIcdd amyE*::pMSAB	This study
QM301	HC11 *amyE*::pMSANMF	This study
Plasmids		
pUC19	Ap^r	Yanisch-Perron et al. (38)
pDH32	Ap^r Cm^r *amyE* front *amyE* back *lacZ*	Grandoni et al. (8)
pFL32	Ap^r *rpoE* gene in *Xba*I-*Hin*dIII sites of pUC19	López de Saro et al. (17)
pMutin	Ap^r Em^r	Vagner et al. (34)
pJH4133	Cm^r, contains *pyrG* gene	Trach et al. (32)
pJH4521	Ap^r Cm^r, *pyrG* gene with Cm insertion	Trach et al. (32)
pCm::Er	Ap^r Em^r	Steinmetz and Richter (30)
pHV502	pMutin with a 2.4-kb *Bcl*I deletion	This study
pMX	186 bp of *Hin*dIII-*Bam*HI fragment of *cdd* gene inserted into *Hin*dIII-*Bam*HI-digested pHV502	This study
pUCAN	*Eco*RI (−96)-*Sac*I (+20) PCR fragment inserted into pUC19 digested with *Eco*RI and *Sac*I	This study
pUCANMF	*Sac*I (+30)-*Bam*HI (+218) PCR fragment inserted into pUCAN digested with *Sac*I and *Bam*HI	This study
Integration plasmids		
pMSAF	*Eco*RI (−96)-*Bam*HI (+218) PCR fragment inserted into pDH32 digested with *Eco*RI and *Bam*HI	This study
pMSAB	*Eco*RI (−96)-*Bam*HI (+36) PCR fragment inserted into pDH32 digested with *Eco*RI and *Bam*HI	This study
pMSCD	*Eco*RI (+57)-*Bam*HI (+110) PCR fragment inserted into pDH32 digested with *Eco*RI and *Bam*HI	This study
pMSAD	*Eco*RI (−96)-*Bam*HI (+110) PCR fragment inserted into pDH32 digested with *Eco*RI and *Bam*HI	This study
pMSAH	*Eco*RI (−96)-*Bam*HI (+80) PCR fragment inserted into pDH32 digested with *Eco*RI and *Bam*HI	This study
pMSANMF	0.32-kb *Eco*RI-*Bam*HI fragment of pUCANMF in pDH32	This study

RESULTS

Characterization of *pyrG* transcripts. A map of the *B. subtilis* genome in the region surrounding *pyrG* (16, 32) is shown in Fig. 2A. The *pyrG* gene lies immediately downstream of the *rpoE* gene and is transcribed in the same direction. The next gene downstream of *pyrG* is *ywjG*, a gene of unknown function transcribed in the opposite direction. Examination of the DNA sequence of the intercistronic region between *rpoE* and *pyrG* (Fig. 2B) revealed a reasonable σ^A-dependent promoter sequence upstream of a possible factor-independent transcription terminator sequence, which presumably functions as the terminator for the *rpoE* gene. The site of initiation of *pyrG* transcription was determined by primer extension analysis using two single-stranded deoxyoligonucleotide primers. Primer B was complementary to mRNA from the *pyrG* coding region and downstream from the terminator sequence, whereas primer C was complementary only to an mRNA sequence upstream of the terminator (Fig. 2B).

Template RNA for primer extension reactions using both primer B and primer C was extracted from HC11 (*pyrB*::*spec*)

cells grown in the presence of 200 μg of cytidine per ml, which represses *pyrG* expression, and from HC11 cells grown in the presence of 100 μg of orotate per ml, a poor pyrimidine source that causes severe pyrimidine starvation (19). For primer extension reactions using primer B, RNA was also extracted from DB104 *pyrG*::*erm* cells grown in the presence of 10 μg of cytidine per ml plus 50 μg of uridine per ml. As shown below for experiments with strain QM206 in Table 3, this is a second method to derepress *pyrG* without resorting to starvation of a pyrimidine auxotroph.

In all cases where a primer-extended product was detectable, the lengths of the extended reverse transcripts from both primers mapped the major site of transcription initiation to the G residue indicated as +1 in Fig. 2B (Fig. 3). For primer extension reactions using primer B (located downstream of the terminator), both methods used to derepress *pyrG* expression led to equal amounts of primer-extended product (Fig. 3, right, lanes 1 and 2), whereas RNA extracted from cells grown under conditions that repress *pyrG* gave only traces of primer-extended product (Fig. 3, right, lane 3). This result suggests that

TABLE 2. Sequences of deoxyoligonucleotides used in this study

Primer	Nucleotide sequence[a]	Coordinate(s)[b]
Deletion analysis		
pyrG-A	CCC<u>GAATTC</u>GACTATGATGATGAAGAAGAGG	−96
pyrG-B	TGAAAG<u>GGATCC</u>TAACGTACTATGTTCTC	+36
pyrG-C	CAAG<u>GAATTC</u>AAAGGGAGCTTTCTTATTTTCACCC	+57
pyrG-D	CGGG<u>GGATCC</u>TTTTAAATGATTTATAAGAAAAATGAG	+110
pyrG-F	CC<u>GGATCC</u>AGGATACAACTCCCCCGGTTAC	+218
pyrG-H	CCCC<u>GGATCC</u>GGTGAAAATAAGAAAGCTC	+80
Mutant construction		
cddHindIII	GGC<u>CAAGCTT</u>GGAGCCGCTCTTCTTACC	2610535–2610518
cddBamHI	CGC<u>GGATCC</u>GGCTCCGCACGGAGATACTGG	2610370–2610350
pyrG-M	GCC**<u>GAGCTCATT</u>**TACGTTATGCTCCCTTTCAAG	+30
pyrG-N	CGC**<u>GAGCTC</u>**CTCTTCGTTTTTGAAGAGCC	+20
Primer extension		
Primer C	CGTACTATGTTCTCTCTTCG	+33
Primer B	GTGAGGATACAACTCCCCCGG	+221
Northern blotting		
pyrG-O	CCGG<u>GGATCC</u>GACGCCACCTGCATGCCC	+1341
pyrG-P	GGT<u>ACTGCAG</u>GAGACATCGAATCACTGCC	+608
rpoE-A	GCG<u>GAATTC</u>GCCGCTTCCTGGCGCTTTCTG	3811920–3811900
rpoE-B	CCTCTTCTTCATCATCATAGTCTTC	3811630–3811606
RT-PCR		
pyrG-Q	GACTATGATGATGAAGAAGAGG	−96

[a] Underlining indicates the position of restriction sites; boldface indicates nucleotides that differ from the wild-type sequence.
[b] Position of the 5′-proximal nucleotide of the primer, except for primers cddHindIII, cddBamHI, rpoE-A, and rpoE-B, for which the nucleotide numbering of the *B. subtilis* genome sequence is used.

repression by cytidine acts by increasing transcription termination at the terminator that lies just downstream from the *pyrG* promoter. For primer extension reactions using primer C (located upstream of the terminator), RNA from cells grown under both repressing and derepressing conditions yielded approximately equal amounts of primer-extended products (Fig. 3, left, lanes 1 and 2), as expected if repression is mediated by the terminator downstream from the primer site.

For cells grown under derepressing conditions, a ladder of somewhat longer primer-extended products (1 to 10 nucleotides [nt] longer than the primary extended product) was clearly observed with primer C (Fig. 3, left, lane 2) and possibly also with primer B (Fig. 3, right, lanes 1 and 2). This observation raised the possibility that some *pyrG*-containing transcripts might originate from the upstream *rpoE* promoter, i.e., that under derepressing conditions some *rpoE-pyrG* bicistronic transcripts are formed. Alternatively, the longer primer-extended products seen with primer C could have resulted from extension of the extreme 3′ end of *rpoE* transcripts if they end at the terminator in the *pyrG* 5′ leader. In that case, the laddering of products would suggest that the *rpoE* transcripts are partially degraded.

The length of *pyrG* and *rpoE* transcripts was probed further by Northern hybridization analysis. Bulk RNA was isolated from HC11 cells grown with cytidine and with orotate, which are repressing and derepressing conditions for *pyrG*. Probes designed to hybridize specifically to transcripts from the *pyrG* and *rpoE* coding regions (Fig. 2A) detected transcripts that were 1.8 and 0.7 knt in length, respectively (Fig. 4). These are the sizes expected for separate *pyrG* and *rpoE* mRNAs. The abundance of the *rpoE* transcripts was not affected by pyrimi-

dine starvation, but the *pyrG* transcripts were much more abundant under these conditions (Fig. 4). This observation indicates that most or all of the *pyrG* transcripts whose abundance is regulated by cytidine originate from the promoter we have mapped to the *rpoE-pyrG* intercistronic region. In no case was a transcript of 2.5 knt, corresponding to a full-length *rpoE-*

TABLE 3. Regulation of *B. subtilis pyrG-lacZ* fusions by pyrimidines

Strain	Genetic background	Addition(s) to minimal medium[a]	Doubling time (min)	β-Galactosidase activity (Miller units)
QM201	Wild type	None	36	68 ± 3
		Urd, Ura	38	65 ± 7
		Cyd	36	50 ± 2
QM202	Δ*pyrR*	None	47	50 ± 1
		Urd, Ura	48	50 ± 2
		Cyd	45	40 ± 4
QM203	Δ*pyrDII*	None	58	110 ± 15
		Urd, Ura	37	55 ± 3
		Cyd	38	40 ± 4
QM204	Δ*pyrDIIcdd*	None	66	130 ± 8
		Urd, Ura	38	70 ± 8
		Cyd	58	17 ± 3
QM205	*pyrB::spec*	Orotate	85	830 ± 190
		Urd, Ura	39	55 ± 8
		Cyd	38	45 ± 8
QM206	*pyrG::erm*	Cyd	48	440 ± 8
		Cyd, 10 μg/ml	88	700 ± 75
		Cyd, 10 μg/ml; Urd	180	1,900 ± 60
		Cyd, 10 μg/ml; Ura	101	1,300 ± 120

[a] Unless specified, cytidine (Cyd) was used at 200 μg/ml, uridine (Urd) was used at 50 μg/ml, and uracil (Ura) was used at 50 μg/ml.

A

B

```
...GACTATGATGATGAAGAAGAGGAAATTAAATAGTATCAGATTTCAT
                                    rpoE translation stop
CTTCAAAACGATCTTGACTTTCATAGTCGAACTATGTAGTATGTATTTTG
                 -35                        -10
+1
GGCTCTTCAAAAACGAAGAGAGAACATAGTACGTTATGCTCCCTTTCAAG
                                           Primer C
AAATTGAAAGGGAGCTTTCTTATTTTCACCCCTCATTTTTCTTATAAATC

ATTTAAAAGGCTAAATGATTTTTTATAAAATAGTACATTTTAAAAATGTA

GCTAAGAGCGAAGAGAGGAGCAAACGAAATGACGAAATATATTTTTGTAA
                     RBS          pyrG translation start
CCGGGGGAGTTGTATCCTCAC...
    Primer B
```
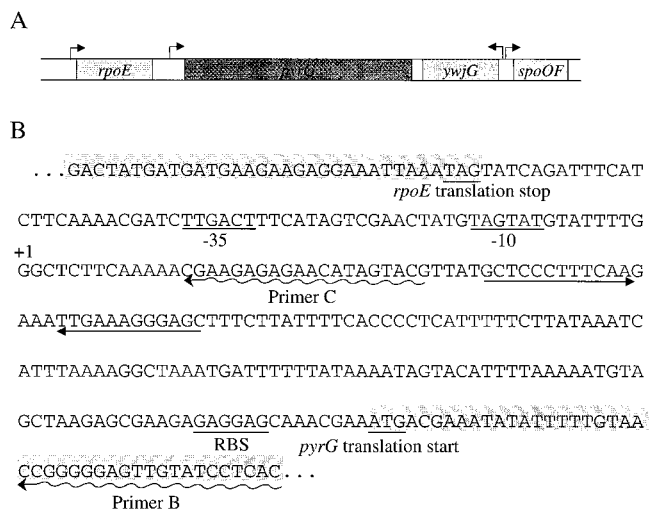
FIG. 2. (A) Structure of the *rpoE-pyrG* region of the *B. subtilis* chromosome. Shaded bars indicate open reading frames. The genes shown are described in the text. Arrows indicate the location and direction of transcription of putative promoters for the genes. (B) Nucleotide sequence of the *rpoE-pyrG* intercistronic region. Shaded bars denote the 3′ end of the *rpoE* coding region and the 5′ end of the *pyrG* coding region. Translation stop and start codons are underlined, as is the ribosome-binding site (RBS) for *pyrG*. −35 and −10 denote the σ^A recognition sequence for the *pyrG* promoter. Straight arrows denote complementary sequences that form a factor-independent terminator hairpin, and wavy arrows show sequences complementary to primers B and C used for primer extension experiments in this work (see Fig. 3).

pyrG bicistronic transcript, detected. However, the *pyrG* transcripts show evidence of considerable degradation, and the presence of a small amount of hybridizing material larger than 1.8 knt may indicate that an *rpoE-pyrG* transcript, if one was formed, could have been degraded under the conditions used.

The question of *rpoE-pyrG* cotranscription was examined further by RT-PCR analysis. RNA from derepressed cells (strain HC11 growth with orotate) was used as a source of *pyrG* mRNA template for RT-PCR in which primer B or primer C (Fig. 2B) and a primer complementary to the 3′ end of the *rpoE* coding region (pyrG-Q) (Table 2) were used for amplification. RT-PCR products of the expected sizes were obtained with primer C but not with primer B (data not shown). This result indicates that *rpoE* transcripts terminate at or very close to the terminator located in the *pyrG* 5′ leader, but no evidence was found for transcripts that include both *rpoE* and *pyrG* coding sequences.

Regulation of *pyrG-lacZ* expression by cytidine nucleotides. We constructed a series of strains in which the entire *rpoE-pyrG* intercistronic region was fused to a *lacZ* reporter gene and the fusion was integrated in a single copy into the chromosomes at the *amyE* locus of several *B. subtilis* strains. These fusions allowed us to study regulation of *B. subtilis pyrG* expression by supplementation of the growth medium with pyrimidine nucleotides or cultivation of the bacteria under conditions of pyrimidine starvation. The *lacZ* reporter gene permitted *pyrG* expression to be readily determined from β-galactosidase assays, whereas we were unable to assay CTP synthetase activity reliably in crude extracts of *B. subtilis* cells. When the *pyrG-lacZ* fusion was integrated into a wild-type (strain DB104) background and the cells were grown on minimal medium with or without pyrimidines, a small but statistically reliable repressive effect of cytidine was observed (Table 3). Cells grown with cytidine expressed 25 to 30% lower levels of β-galactosidase than cells grown without supplementation. Uracil and uridine did not cause significant repression.

When these experiments were repeated with the *pyrG-lacZ* fusion integrated into a strain with an in-frame deletion of the *pyrR* gene (33), expression levels were reduced by about 30% compared to expression in wild-type cells and exhibited only very small repressive effects of cytidine. Since deletion of the *pyrR* gene has been shown to lead to very high, constitutive overexpression of the genes of the *pyr* operon (33), the low expression of the *pyrG-lacZ* fusion in the Δ*pyrR* strain indicates that *pyrR* is not involved in regulation of *pyrG* expression. The reduced level of *pyrG* expression in the Δ*pyrR* strain probably results from very high levels of intracellular pyrimidine nucleotides (including CTP) in this strain (21, 33).

Regulation of *pyrG* expression could be demonstrated more convincingly by integrating the *pyrG-lacZ* fusion into strains that could be starved for pyrimidines. A derivative of DB104 with an in-frame deletion of the *pyrDII* gene grows slowly in the absence of pyrimidines and exhibits derepressed *pyr* genes because of reduced intracellular pyrimidine nucleotide levels (14). Expression of *pyrG-lacZ* was elevated 1.7-fold in a Δ*pyrDII* background (strain QM203) relative to the wild-type strain QM201 (Table 3). Addition of pyrimidines to this strain brought about repression of *pyrG*, twofold repression by uracil plus uridine, and almost threefold repression by cytidine. Since the repressive effects of cytidine might be masked by deamination of this nucleoside by cytidine deaminase (*cdd*), *pyrG-lacZ* expression was also determined in a Δ*pyrDIIcdd* background (strain QM204). Repression by uracil plus uridine was not altered by the *cdd* mutation, but cytidine became a more effective repressor (seven- to eightfold repression). These observations suggest that a cytidine nucleotide is the most effective metabolite for repression of *pyrG* and that uridine nucleotides may act only via conversion to cytidine nucleotides. The largest derepression of *pyrG-lacZ* expression observed in our studies was obtained by growth of a pyrimidine auxotroph, strain QM205 (*pyrB::spec*) (11), on orotate, which is taken up slowly by the cells and results in slow growth and highly derepressed *pyr* gene expression (19). As seen in Table 3, *pyrG-lacZ* was expressed at very high levels in the *pyrB::spec* background when the cells were starved for pyrimidines by growth on orotate and was repressed 20-fold when the cells were grown with cytidine. Growth of strain QM205 with excess uracil plus uridine brought about 12-fold repression.

The foregoing experiments demonstrated repression of *pyrG* expression by pyrimidines in the growth medium and suggested that cytidine nucleotides were more effective than uridine nucleotides as corepressors, but they did not allow the cytidine and uridine nucleotide pools to be manipulated separately. This was accomplished by studying *pyrG-lacZ* expression when the fusion was integrated into a strain in which the normal chromosomal *pyrG* gene was disrupted by insertion of an erythromycin resistance gene. This strain, QM206, was a cytidine auxotroph; uracil, uridine, and cytosine did not support growth. Interestingly, this strain had a normal *cdd* gene, which demonstrates that in *B. subtilis*—unlike enteric bacteria (23)—cytidine deaminase is not sufficiently active to prevent growth
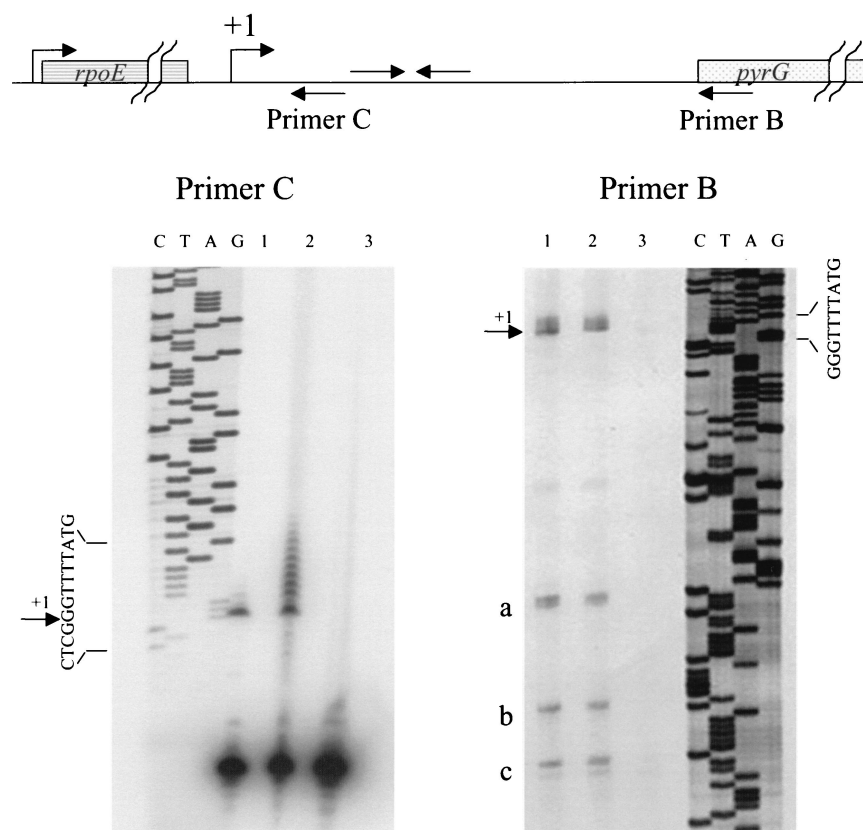
FIG. 3. Identification of the start site of *pyrG* transcription by primer extension. (Left) Lane 1, 10 μg of total RNA from strain HC11 grown with 200 μg of cytidine per ml was used; lane 2, 10 μg for total RNA from strain HC11 grown with 100 μg of orotate per ml was used; lane 3, no primer extension (primer C only was subjected to electrophoresis). The left side of the panel shows the results of dideoxy sequencing of the *rpoE-pyrG* region with primer C to allow identification of the end of the primer-extended product. (Right) Lane 1, 10 μg of total RNA from strain DB104 *pyrG::erm* grown on minimal medium with 10 μg of cytidine and 50 μg of uridine per ml was used; lane 2, 10 μg of total RNA from strain HC11 grown with 100 μg of orotate per ml was used; lane 3, 10 μg of total RNA from strain HC11 grown with 200 μg of cytidine per ml was used. Prematurely terminated primer extension products are indicated by a, b, and c; product a probably results from blockage of reverse transcriptase at the terminator hairpin, and products b and c occur in A- and U-rich regions of the reverse transcriptase template. The right side of the panel shows the results of dideoxy sequencing of the *rpoE-pyrG* region with primer B.

of a *pyrG* strain on cytidine. Strain QM206 grew more slowly with 10 than with 200 μg of cytidine per ml; cytidine limitation resulted in derepression of an integrated *pyrG-lacZ* fusion (Table 3). Addition of 50 μg of uridine per ml did not increase the slow growth brought about by 10 μg of cytidine per ml; in fact, it caused the cells to grow more slowly and resulted in further derepression of *pyrG*. This effect can be explained by the fact that cytidine and uridine are known to share a common uptake protein in *B. subtilis*, NupC (15, 28). Thus, addition of uridine results in competitive inhibition of cytidine uptake, decreased pools of intracellular cytidine nucleotides, and further derepression of *pyrG*. Uracil, which is believed to be taken up by the PyrP carrier in *B. subtilis* (33), caused modest inhibition of growth and *pyrG* derepression. These experiments indicate that *pyrG* expression is regulated largely, if not entirely, by intracellular cytidine nucleotide pools, because the highest expression was obtained in *pyrG::erm* cells that were the most severely starved for cytidine but would be predicted to have high uridine nucleotide pools.

Mutational analysis of the *pyrG* leader indicates an antitermination mechanism for repression but does not identify an antiterminator in the *pyrG* RNA. Additional insight into the

elements present in the *rpoE-pyrG* intercistronic region that are important for *pyrG* expression and its repression by cytidine was obtained by characterizing the expression of a series of deletions of the QM205 *pyrG-lacZ* fusion that was studied for Table 3. The parent fusion and the deletions shown in Fig. 5 were integrated into strain HC11 (*pyrB::spec*) and grown under repressing and derepressing conditions, i.e., in minimal medium with either 200 μg of cytidine or 100 μg of orotate per ml, respectively. Normal expression and regulation were obtained with all fusion-integrant strains that contained sequences from the 3′ end of *rpoE* to +80 in the *pyrG* leader transcript. However, further deletion of *pyrG* leader sequences from +37 to +80, which specify a putative factor-independent transcription terminator, led to highly derepressed *pyrG* expression, which was not reduced by cytidine in the medium (Fig. 5, strain QM104). The threefold further increase in expression in cells of this strain that were starved by growth on orotate may be a nonspecific effect of this extreme starvation, as has been previously observed for the *pyr* operon (19). This conclusion is supported by the observation that an alternative mode of *pyrG* derepression, growth of a Δ*pyrDIIcdd* strain without pyrimidines, yielded only 1.6-fold derepression in the
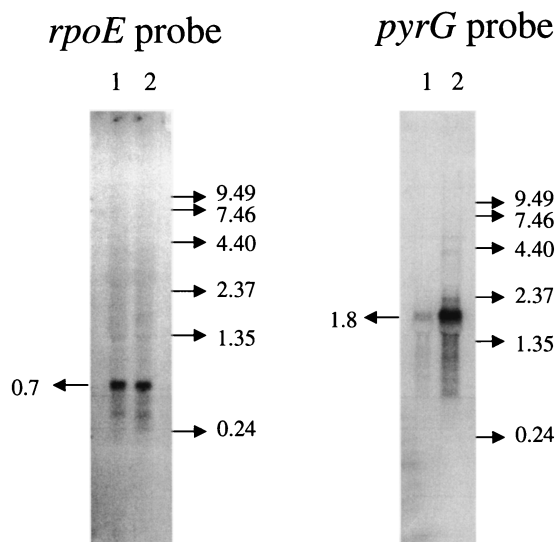
FIG. 4. Northern hybridization analysis of *rpoE* and *pyrG* transcripts. Total RNA (10 μg) from strain HC11 grown on minimal medium with 200 μg of cytidine per ml (lane 1) or 100 μg of orotate per ml (lane 2) was subjected to electrophoresis, electroblotted onto nylon membranes, and hybridized with ^{32}P-labeled deoxyoligonucleotide probes. The positions of RNA size standards (in kilonucleotides) are on the right of each panel.

QM234 strain containing the same deletion of the terminator but 8-fold derepression in strain QM204 (Fig. 5). When a downstream segment from the *rpoE-pyrG* intercistronic region, +57 to +110, was fused to *lacZ* and integrated into strain HC11, no detectable β-galactosidase was expressed. These findings support the conclusions from the primer extension experiments that the only active *pyrG* promoter lies upstream of transcription terminator that is predicted to lie between nt +38 and +70 of the *pyrG* transcript leader (Fig. 2B). Furthermore, the repression of *pyrG* expression by cytidine requires

the presence of this terminator. This leads us to suggest that termination at this site is efficient when cytidine nucleotides are abundant in the cell and that cytidine starvation suppresses termination.

What mechanism could account for regulation of termination in the *pyrG* 5′ leader by cytidine nucleotides? Clearly, some mechanism for preventing transcription termination must act when the cytidine nucleotide pool is low. We searched the sequence of the 5′ leader with the MULFOLD program (12, 13, 39) for a possible RNA antiterminator hairpin and identified only a single, relatively weak alternative RNA structure that would prevent the more stable terminator hairpin from forming (Fig. 6). However, a mutagenesis experiment in which nucleotides 21 through 29 were replaced with nucleotides that cannot base-pair to form the putative antiterminator hairpin in a *pyrG-lacZ* fusion integrant gave regulation of β-galactosidase expression by cytidine that was similar to that of the native *pyrG-lacZ* fusion integrant (Fig. 6).

DISCUSSION

Prior to the present study, little was known about the regulation of *pyrG* expression in *B. subtilis*. Our results demonstrate that *pyrG* transcription is regulated by cytidine nucleotides, although the repressive effects of cytidine are very small unless the cells are starved for pyrimidines and are enhanced when the gene encoding cytidine deaminase is inactivated. This suggests that the intracellular level of the regulatory metabolite formed by de novo biosynthesis is high enough to almost fully repress *pyrG*. Experiments with a strain in which conversion of UTP to CTP was blocked by a *pyrG* disruption allowed us to starve the cells for cytidine nucleotides while providing abundant uridine nucleotides. Under these conditions *pyrG* was fully derepressed, which indicated that the cytidine nucleotides are the repressing metabolites for this gene. While we have not measured nucleotide pools directly in our experiments, it

FIG. 5. Deletion analysis of *pyrG-lacZ* fusion integrants. The portions of the *rpoE-pyrG* intercistronic region shown were fused to *lacZ* in pDH32 and integrated into the *B. subtilis* chromosome at *amyE* in the indicated strains. The cells were grown under repressing (+cytidine) or derepressing (+orotate or −cytidine) conditions and harvested during exponential growth. The β-galactosidase activities of the cells were assayed to determine the degree of *pyrG* expression.

Terminator   Antiterminator?

```
              A  A
            G     A
             A U
             A U
             C G
             U A
  A A  A     U A                            A  C
 A    C      U A                          U     G
  A C G      C G                 A A  A    G U
   U A   A G U    C G           A    C     A U
   U A   U    A   C G            A C G     U A
   C G    A  C    U A             U A      A U
   U A   C G      C G             U A      C G
   U A    A U     C G             C G      A  C
 GGC GA G A U  AU G CUUUCUUAUUUUCACC        U A      A U
 +1          +38      +70                 GGC G A  G  CCCUUUCAAGAAA
                                          +1      +21
```

	Strain	Genetic background	+ Cytidine	+Orotate	Ratio
	QM205	*pyrB::spec*	46 ± 8	830 ± 190	18
	QM301	*pyrB::spec*	14 ± 3	590 ± 53	42

FIG. 6. Test of the role of a possible antiterminator hairpin in the *pyrG* 5′ leader in regulation of *pyrG* expression. (Top) Two possible ways of folding the *pyrG* 5′ leader RNA as predicted by MULFOLD. On the left is the more stable predicted structure, which includes a factor-independent transcription terminator. On the right is a less stable alternative structure in which a putative antiterminator hairpin could form. The nucleotides in boldface are those present in the native sequence (QM205) which were replaced by the sequence 5′-GAGCUCAUU-3′ in the mutant strain QM301. Sequencing of the mutant DNA confirmed the correct structure, except that the nucleotide at +5, which is a C in QM205, had also been replaced by a U in QM301. (Bottom) Results of β-galactosidase assays determining the levels of expression of the *pyrG-lacZ* fusions in QM205 and QM301 under repressing (+cytidine) and derepressing (+orotate) conditions. Cells were grown in the minimal medium described by Lu et al. (19).

seems most probable to us that the actual regulatory metabolite is CTP, since this nucleotide is the product of the enzyme encoded by *pyrG* and CTP is the cytidine nucleotide used directly in biosynthetic pathways.

The most abundant *pyrG* transcripts found in *B. subtilis* cells originate from a promoter which we identified in the *rpoE-pyrG* intercistronic region, and these became more abundant in cells that were starved for pyrimidines. Bicistronic *rpoE-pyrG* transcripts were not detected, however. Most *rpoE* transcripts were the size of monocistronic transcripts, and their abundance was not altered by starvation for pyrimidines. This is consistent with the report of López de Saro et al. (18) that the *rpoE* promoter is expressed at substantial levels under all conditions examined.

The most important new finding in our work is that *B. subtilis pyrG* expression is regulated by a factor-independent transcription terminator located in the *pyrG* 5′ leader downstream from the *pyrG* promoter. Termination at this site is regulated by cytidine nucleotides over an 8- to 10-fold range if the effects on *pyrG-lacZ* fusion integrants can be taken to reflect levels of *pyrG* mRNA. Evidence for the role of this terminator was of two kinds. First, primer-extended transcripts originating from a primer upstream of the terminator (primer C in Fig. 3) were equally abundant in cells grown under repressing and derepressing conditions, whereas primer-extended transcripts originating from a primer downstream of the terminator (primer B in Fig. 3) were much less abundant in cells grown with excess cytidine. More direct evidence was provided by deletion analysis of the *pyrG* leader region in *pyrG-lacZ* transcriptional fusions (Fig. 5).

The presence of a regulated transcription terminator upstream of the coding region of the gene being regulated is the hallmark of an attenuation system. In two of the best-studied cases of biosynthetic operons regulated by attenuation in *B. subtilis*, the *trp* operon (2) and the *pyr* operon (31), a more stable antiterminator hairpin forms in the leader RNA before the terminator hairpin can form. This condition prevents termination and allows expression of the downstream genes. In the presence of an end product of the operon, a regulatory protein—*trp* RNA-binding attenuation protein plus tryptophan in the case of the *trp* operon and PyrR plus UMP or UTP in the case of the *pyr* operon—binds to a specific site in the 5′ stem of the antiterminator hairpin and destabilizes it, allowing formation of the terminator.

In other antitermination systems, the terminator hairpin is the most stable secondary structure in the leader mRNA, and antitermination is brought about by the binding of a regulatory protein to sequences upstream of the terminator, which prevents terminator formation. In some cases, such as the *E. coli bgl* operon (1) and the *B. subtilis sacB* operon (20, 35), the regulatory protein, BglG or SacY, respectively, binds to an RNA antiterminator hairpin that overlaps the sequence of the terminator hairpin. Antitermination in the lambdoid phages is mechanistically similar but involves direct interactions with RNA polymerase and the Nus proteins (10). In other cases, such as the *nasF* operon of *Klebsiella* (4), there is no identifiable antiterminator hairpin that overlaps the terminator. Instead, the antiterminator protein NasR appears to bind to a hairpin that lies upstream of the terminator hairpin and is separated from it by a 9-nt linker (4). The *pyrG* leader RNA resembles the

```
Bsu   GGGCUC---32nt----GCUCCC---16nt---GGGAGC-polyU
Bha   GGGCUA---39nt----GCCCCC--- 9nt---GGGAAA-8nt-polyU
Ban   GGGCUC---49nt----GCUCCC---23nt---GGGAGC-2nt-polyU
Bst   GGGCUC---21nt----GCUCCC---13nt---GCGGAGC-1nt-polyU
Efa   GGGCAC---35nt----GCUCCC---15nt---GGGAGC-polyU
Spy   GGGCAC---22nt----GCUCUC--- 9nt---GGGGGC-2nt-polyU
Spn   GGGCUC---17nt----GCUCCC--- 9nt---GGGAGC-2nt-polyU
Sau   GGGCUC---32nt----GCUCCC---18nt---GGGAGC-1nt-polyU
Llac  GGGCAC---33nt----GCUCCC--- 5nt---GGGAGC-2nt-polyU
Lcre  GGGCAC---33nt----GCUC----- 4nt-----GAGC-2nt-polyU
```

FIG. 7. Conserved sequences in the 5′ untranslated leader regions of the *pyrG* genes from 10 gram-positive bacteria. For each sequence the first conserved segment is located 7 nt downstream from a reasonable −10 sequence for a promoter and is likely to be at or near the 5′ end of the *pyrG* mRNA. The second and third conserved sequences are complementary and are predicted to form part of the stem of a rho-independent transcription terminator that serves as the *pyrG* attenuator, which is followed by several U residues (polyU). Sequences and their sources: Bsu, *B. subtilis* (16); Bha, *Bacillus halodurans*, GenBank accession no. AP001520; Ban, *B. anthracis*, TIGR; Bst, *B. stearothermophilus*, TIGR; Efa, *E. faecalis*, TIGR; Spy, *Streptococcus pyogenes*, GenBank accession no. AE006614; Spn, *S. pneumoniae*, TIGR; Sau, *Staphylococcus aureus*, GenBank accession no. AP003364; Llac, *Lactococcus lactis* subsp. *lactis*, GenBank accession no. AE006284; Lcre, *L. lactis* subsp. *cremoris*, GenBank accession no. AJ010153.

latter group of antitermination systems because the terminator structure is predicted to be the most stable secondary structure. We suggest that a hypothetical regulatory protein binds upstream of this terminator when the level of a cytidine nucleotide, most likely CTP, is low and that the binding of CTP at high concentrations causes the protein to dissociate from the *pyrG* mRNA, allowing transcriptional termination. The RNA sequences of the *pyrG* leader upstream of its terminator have no homology to any of the known antitermination systems. We searched the sequence of the *pyrG* 5′ leader for antiterminator hairpin structures that overlap with the terminator and identified only one candidate (Fig. 6). However, mutation of the sequence of this region so as to prevent the antiterminator from forming did not reduce the ability of *pyrG* to be repressed by cytidine.

A comparison of the *pyrG* 5′ leader sequences from 10 different gram-positive bacteria suggests that the mechanism for *pyrG* regulation we have identified is found in these other bacteria as well (Fig. 7). All of the leader RNA sequences are capable of forming transcription terminator structures. Furthermore, three sequence segments are conserved in the RNA of the *pyrG* leaders. The first of these, GGGC(U/A)C, is consistently located at the very 5′ end of the *pyrG* transcript. In some cases this sequence may form part of the stem of a hairpin structure, as suggested for the *B. subtilis pyrG* leader (Fig. 6), but this did not appear to always be the case. Two additional conserved segments were observed in each of the leaders, typically GCUCCC and GGGAGC; these were consistently base-paired to form the base of the stem of a terminator hairpin, as shown for *B. subtilis pyrG* in Fig. 6. Only in the case of *Lactococcus lactis* subsp. *cremoris* is the terminator so truncated that its formation is questionable. The presence of these conserved sequence elements in the gram-positive *pyrG* leaders provides a hint that they are important for regulation of expression, either by serving as recognition elements for a regulatory protein or by participation in a higher-order RNA folding structure that we have not yet identified.

An unusual feature of our model is that the *pyrG* attenuator also functions as the transcription terminator for the upstream *rpoE* gene, so that under conditions of cytidine starvation some *rpoE-pyrG* bicistronic transcripts should be formed. Other instances of transcription terminators that appear to also function as attenuators for downstream genes have been described for the *B. subtilis gltX-cysES* (7) and *acsA-tyrS* (9) operons, but in the former case there is not a second promoter immediately upstream of the terminator. From our observations it appears that the majority of *pyrG* transcripts originate from the *pyrG* promoter, not the *rpoE* promoter, and, furthermore, that any bicistronic transcripts that may be formed are too unstable in vivo to be detected. Evidence for the cleavage of the *B. subtilis gltX-cysES* (25) and *acsA-tyrS* (5) transcripts at sites near the intercistronic terminators has been presented. Such cleavage may be a general feature of such transcripts.

Our hypothesis for the regulation of *pyrG* by an antitermination mechanism obviously needs further experimental testing. Such work is currently under way in our laboratory.

REFERENCES

1. **Amster-Choder, O., and A. Wright.** 1993. Transcriptional regulation of the *bgl* operon of *Escherichia coli* involves phosphotransferase system-mediated phosphorylation of a transcriptional antiterminator. J. Cell. Biochem. **51:** 83–90.
2. **Antson, A. A., E. J. Dodson, G. Dodson, R. B. Greaves, X.-P. Chen, and P. Gollnick.** 1999. Structure of the *trp* RNA-binding attenuation protein, TRAP, bound to RNA. Nature **401:** 235–242.
3. **Asahi, S., M. Doi, Y. Tsunemi, and S. Akiyama.** 1989. Regulation of pyrimidine nucleotide biosynthesis in cytidine deaminase-negative mutants of *Bacillus subtilis*. Agric. Biol. Chem. **53:** 97–102.
4. **Chai, W., and V. Stewart.** 1999. RNA sequence requirements for NasR-mediated, nitrate-responsive transcription antitermination of the *Klebsiella oxytoca* M5a1 *nasF* operon leader. J. Mol. Biol. **292:** 203–216.
5. **Condon, C., H. Putzer, and M. Grunberg-Manago.** 1996. Processing of the leader mRNA plays a major role in the induction of *thrS* expression following threonine starvation in *Bacillus subtilis*. Proc. Natl. Acad. Sci. USA **93:** 6992–6997.
6. **Contente, S., and D. Dubnau.** 1979. Characterization of plasmid transformation in *Bacillus subtilis*: kinetic properties and the effect of DNA conformation. Mol. Gen. Genet. **167:** 251–258.
7. **Gagnon, Y., R. Breton, H. Putzer, M. Pelchat, M. Grunberg-Manago, and J. Lapointe.** 1994. Clustering and co-transcription of the *Bacillus subtilis* genes encoding the aminoacyl-tRNA synthetases specific for glutamate and for cysteine and the first enzyme for cysteine biosynthesis. J. Biol. Chem. **269:** 7473–7482.
8. **Grandoni, J. A., S. B. Fulmer, V. Brizzio, S. A. Zahler, and J. M. Calvo.** 1993. Regions of the *Bacillus subtilis ilv-leu* operon involved in regulation by leucine. J. Bacteriol. **175:** 7581–7593.
9. **Grundy, F. J., D. A. Waters, T. Y. Takova, and T. M. Henkin.** 1993. Identification of genes involved in utilization of acetate and acetoin in *Bacillus subtilis*. Mol. Microbiol. **10:** 259–271.
10. **Henkin, T. M.** 1996. Control of transcriptional termination in prokaryotes. Annu. Rev. Genet. **30:** 35–57.
11. **Hu, P., and R. L. Switzer.** 1995. Evidence for substrate stabilization in regulation of the degradation of *Bacillus subtilis* aspartate transcarbamylase in vivo. Arch. Biochem. Biophys. **316:** 260–262.
12. **Jaeger, J. A., D. H. Turner, and M. Zuker.** 1989. Improved predictions of secondary structures for RNA. Proc. Natl. Acad. Sci. USA **86:** 7706–7710.
13. **Jaeger, J. A., D. H. Turner, and M. Zuker.** 1989. Predicting optimal and

suboptimal secondary structure for RNA. Methods Enzymol. **183:**281–306.

14. **Kahler, A. E., and R. L. Switzer.** 1996. Identification of a novel gene of pyrimidine nucleotide biosynthesis, *pyrDII*, that is required for dihydrooroate dehydrogenase activity in *Bacillus subtilis*. J. Bacteriol. **178:**5013–5016.

15. **Kloudová, A., and V. Fucik.** 1974. Transport of nucleoside in *Bacillus subtilis*: characteristics of cytidine uptake. Nucleic Acids Res. **1:**629–637.

16. **Kunst, F., N. Ogasawara, I. Moszer, A. M. Albertini, G. Alloni, V. Azevedo, M. G. Bertero, P. Bessieres, A. Bolotin, S. Borchert, R. Borriss, L. Boursier, A. Brans, M. Braun, S. C. Brignell, S. Bron, S. Brouillet, C. V. Bruschi, B. Caldwell, V. Capuano, N. M. Carter, S. K. Choi, J. J. Codani, I. F. Connerton, A. Danchin, et al.** 1997. The complete genome sequence of the Gram-positive bacterium *Bacillus subtilis*. Nature **390:**249–256.

17. **López de Saro, F. J., A. M. Woody, and J. D. Helmann.** 1995. Structural analysis of the *Bacillus subtilis* factor δ: a protein polyanion which displaces RNA from RNA polymerase. J. Mol. Biol. **252:**189–202.

18. **López de Saro, F. J., N. Yoshikawa, and J. D. Helmann.** 1999. Expression, abundance, and RNA polymerase binding properties of the δ factor of *Bacillus subtilis*. J. Biol. Chem. **274:**15953–15958.

19. **Lu, Y., R. J. Turner, and R. L. Switzer.** 1995. Roles of the three transcriptional attenuators of the *Bacillus subtilis* pyrimidine biosynthetic operon in the regulation of its expression. J. Bacteriol. **177:**1315–1325.

20. **Manival, X., Y. Yang, M. P. Strub, M. Kochoyan, M. Steinmetz, and S. Aymerich.** 1997. From genetic to structural characterization of a new class of RNA-binding domain within the SacY/BglG family of antiterminator proteins. EMBO J. **16:**5019–5029.

21. **Martinussen, J., P. Glaser, P. S. Andersen, and H. H. Saxild.** 1995. Two genes encoding uracil phosphoribosyltransferase are present in *Bacillus subtilis*. J. Bacteriol. **177:**271–274.

22. **Miller, J. H.** 1972. Experiments in molecular genetics. Cold Spring Harbor Laboratory, Cold Spring Harbor, N.Y.

23. **Neuhard, J., and P. Nygaard.** 1987. Purines and pyrimidines, p. 445–473. *In* F. C. Neidhardt (ed.), *Escherichia coli* and *Salmonella typhimurium*: cellular and molecular biology, vol. 1. American Society for Microbiology, Washington, D.C.

24. **Nygaard, P., P. Duckert, and H. H. Saxild.** 1996. Role of adenine deaminase in purine salvage and nitrogen metabolism and characterization of the *ade* gene in *Bacillus subtilis*. J. Bacteriol. **178:**846–853.

25. **Pelchat, M., and J. Lapointe.** 1999. In vivo and in vitro processing of the *Bacillus subtilis* transcript coding for glutamyl-tRNA synthetase, serine acetyltransferase, and cysteinyl-tRNA synthetase. RNA **5:**281–289.

26. **Sambrook, J., E. F. Fritsch, and T. Maniatis.** 1989. Molecular cloning: a laboratory manual, 2nd ed. Cold Spring Harbor Laboratory Press, Cold Spring Harbor, N.Y.

27. **Sanger, F., S. Nicklen, and A. R. Coulson.** 1977. DNA sequencing with chain-terminating inhibitors. Proc. Natl. Acad. Sci. USA **74:**5463–5467.

28. **Saxild, H. H., L. N. Andersen, and K. Hammer.** 1996. *dra-nupC-pdp* operon of *Bacillus subtilis*: nucleotide sequence, induction by deoxyribonucleosides, and transcriptional regulation by the *deoR*-encoded DeoR repressor protein. J. Bacteriol. **178:**424–434.

29. **Saxild, H. H., J. H. Jacobsen, and P. Nygaard.** 1995. Functional analysis of the *Bacillus subtilis purT* gene encoding formate-dependent glycinamide ribonucleotide transformylase. Microbiology **141:**2211–2218.

30. **Steinmetz, M., and R. Richter.** 1994. Plasmids designed to alter the antibiotic resistance expressed by insertion mutations in *Bacillus subtilis* through in vivo recombination. Gene **142:**79–83.

31. **Switzer, R. L., R. J. Turner, and Y. Lu.** 1999. Regulation of the *Bacillus subtilis* pyrimidine biosynthetic operon by transcriptional attenuation: control of gene expression by an mRNA-binding protein. Prog. Nucleic Acids Res. Mol. Biol. **62:**329–367.

32. **Trach, K., C. J. W., P. L. D. Piggot, and J. A. Hoch.** 1988. Complete sequence and transcriptional analysis of the *spo0F* region of the *Bacillus subtilis* chromosome. J. Bacteriol. **170:**4194–4208.

33. **Turner, R. J., Y. Lu, and R. L. Switzer.** 1994. Regulation of the *Bacillus subtilis* pyrimidine biosynthetic (*pyr*) gene cluster by an autogenous transcriptional attenuation mechanism. J. Bacteriol. **176:**3708–3722.

34. **Vagner, V., E. Dervyn, and S. D. Ehrlich.** 1998. A vector for systematic gene inactivation in *Bacillus subtilis*. Microbiology **144:**3097–3104.

35. **Van Tilbeurgh, H., X. Manival, S. Aymerich, J.-M. Lhoste, C. Dumas, and M. Kochoyan.** 1997. Crystal structure of a new RNA-binding domain from the antiterminator protein SacY of *Bacillus subtilis*. EMBO J. **16:**5030–5036.

36. **West, T. P., and G. A. O'Donovan.** 1982. Repression of cytidine triphosphate synthetase in *Salmonella typhimurium* by pyrimidines during uridine nucleotide depletion. J. Gen. Microbiol **128:**895–899.

37. **Wilson, K.** 1990. Preparation of genomic DNA from bacteria, p. 2.4.1–2.4.2. *In* F. M. Ausubel, R. Brent, R. E. Kingston, D. D. Moore, J. G. Seidman, J. A. Smith, and K. Struhl (ed.), Current protocols in molecular biology, supplement 9. Greene Publishing Associates and Wiley Interscience, New York, N.Y.

38. **Yanisch-Perron, C., J. Vieira, and J. Messing.** 1985. Improved M13 phage cloning vectors and host strains: nucleotide sequences of the M13mp18 and pUC19 vectors. Gene **33:**103–119.

39. **Zuker, M., and P. Stiegler.** 1981. Optimal computer folding of large RNA sequences using thermodynamics and auxiliary information. Nucleic Acids Res. **9:**133–148.